ISSN: 2277-3754
ISO 9001:2008 Certified
International Journal of Engineering and Innovative Technology (IJEIT)
Volume 4, Issue 1, July 2014

FTIR and thermal studies of gel-grown, lead-iron-mixed levo tartrate crystals

H.O. Jethva*, M.J. Joshi
Crystal Growth Laboratory, Department of Physics, Saurashtra University, Rajkot 360 005, India

Abstract: ***In the present investigation, lead-iron mixed levo tartrate crystals for different compositions of lead and iron were grown by single diffusion gel growth technique in silica hydro gel medium. Long and dendrite type white crystals were obtained. The metallic composition in the crystals was estimated by EDAX. The powder XRD suggested the orthorhombic nature of the grown mixed crystals. The grown crystals were characterized by FTIR spectroscopy and thermal studies. The FTIR spectra revealed the presence of water molecules, O-H, C-H, C-O, C=O and C-C functional groups. The thermo-grams suggested that the crystals were thermally unstable and decomposed into oxide through a single stage of carbonates. DTA curves showed endothermic and exothermic reactions.***

Keywords- **Lead-iron mixed levo tartrate crystals, gel growth, FTIR, powder XRD, TG, DTA.**

I. INTRODUCTION

The metal tartrate compounds find various applications in different fields, for example, application of tartrate ions to treat prostate cancer [1], iron tartrate complex ions play important role as contrast blocks of renal tissues prior to their dehydration [2], iron tartrate is one of the prominent species in apple juice [3], calciphylatic responses of various ferrous tartrate compounds to prevent anemia in animals [4], the potential for iron(III) tartrate to act as a photo activator in light-induced oxidative degradation of white wine [5], ferroelectric, dielectric, optical and thermal properties of calcium tartrate [6], piezoelectric application of cadmium tartrate [7] and the addition of lead tartrate in gasoline to prevent knocking in motors [8]. The gel growth technique is found to be suitable to grow tartrate compound crystals and many authors have reported the growth of metal tartrate crystals [9-12], mixed metal tartrate crystals [13,14] and ternary metal tartrate crystals [15,16] in gel medium. Looking at limited but significant application of iron tartrate and lead tartrate, the present authors have attempted to grow the mixed levo tartrate crystals of two metals i.e., lead and iron, of different proportions and characterize them by Powder XRD, EDAX, FTIR, TG, DTA and DSC.

II. EXPERIMENTAL

The single diffusion gel growth technique was employed for the growth of lead – iron mixed levo tartrate crystals. The silica hydro gel was used as a growth medium. To prepare the gel, a solution of sodium meta silicate of 1.05 specific gravity was acidified by 1 M solution of levo-tartaric acid in such a manner that the pH of the mixture was set at 4.5. The gel solution was poured in to glass test tubes of 15 cm length and 2.5 cm diameter and allowed to set in the gel form. The supernatant solution was poured on the set gel carefully without damaging the gel. The composition of the supernatant was as under.

(I) 1 M, 4 ml $Pb(NO_3)_2$ + 1 M, 6 ml $Fe(NO_3)_2{\cdot}9H_2O$

(II) 1 M, 6 ml $Pb(NO_3)_2$ + 1 M, 4 ml $Fe(NO_3)_2{\cdot}9H_2O$

(III) 1 M, 8 ml $Pb(NO_3)_2$ + 1 M, 2 ml $Fe(NO_3)_2{\cdot}9H_2O$

All the chemicals were AR grade and obtained from Ranbaxy chemicals. The following reaction is expected to occur.

$$(1 - X)Pb(NO_3)_2 + XFe(NO_3)_2{\cdot}9H_2O + H_2C_4H_4O_6 + nH_2O \rightarrow Fe_XPb_{(1-X)}C_4H_4O_6{\cdot}\ nH_2O + 4HNO_3 + 8H_2O + 1/2O_2 \quad (1)$$

Where, X = 0.6, 0.4 and 0.2. Exact value of X is to be determined from EDAX analysis. The amount of HNO_3 produced is very less in comparison to the nutrients being supplied to the growing crystals and hence no major limitation is imposed [9,13,15,16].

The growth was completed within twenty days. The nature of the grown crystals was dendrite type for all the three samples but the growth density of the crystals at the gel - liquid interface and the color were changed as per the composition of the supernatant solutions. Growth of crystals inside the test tubes is shown in fig 1(a-c) for the solution (I), (II) and (III), respectively. The coloration of grown crystals changed from light brown to nearly white on moving from solution I to solution III.

The grown crystals were characterized by different techniques. The EDAX was recorded on Philips XL-30 set up. The Powder XRD patterns were recorded on Philips X'pert MPD by using Cu K_α radiation and the data were analyzed by software powder-x. The FTIR spectra were recorded on Perkin Elmer Spectrum GX spectrophotometer in the range from 400-4000 cm^{-1} in KBr medium. The simultaneous TG, DTA and DSC were conducted on Linseis (STA PT 1600) from room temperature to 700 ^oC at a heating rate of 10 $^oC\ min^{-1}$ in atmosphere of air in standard Al_2O_3 crucible. Various thermodynamic parameters were calculated by using the software TG Evaluation available with the set up.

ISSN: 2277-3754
ISO 9001:2008 Certified
International Journal of Engineering and Innovative Technology (IJEIT)
Volume 4, Issue 1, July 2014

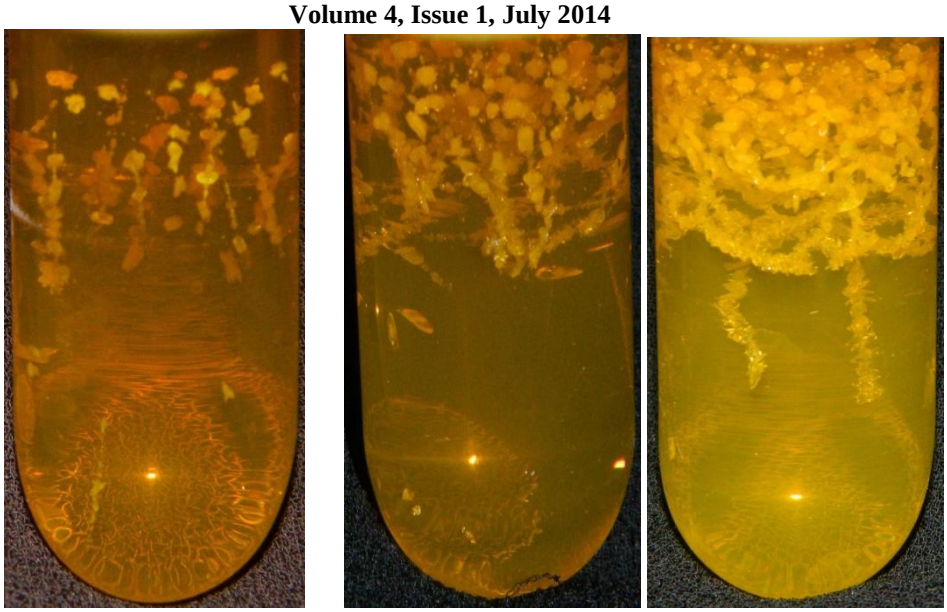

1(a) 1(b) 1(c)

Fig 1. Growth of crystals in test tubes

III. RESULT AND DISCUSSION

The composition of grown crystals was determined by EDAX. It was found 98.93 wt% Pb and 1.07 wt% Fe for sample I, 99.36 wt% Pb and 0.64 wt% Fe for sample II and 99.38 wt% Pb and 0.62 wt% Fe for sample III. The proposed formula for the mixed crystals is $Pb_{98.93}Fe_{1.07}C_4H_4O_6$ nH_2O, $Pb_{99.36}Fe_{0.64}C_4H_4O_6$ nH_2O and $Pb_{99.38}Fe_{0.62}C_4H_4O_6$ nH_2O for samples (I), (II) and (III), respectively. It is found that the presence of lead and iron is not as per expectation from the volume of lead nitrate and ferrous nitrate in the supernatant solution, i.e., lead enters the crystalline lattice readily then iron. The reason can be explained on the basis of hydrated radii. In the solution, Pb^{+2} and Fe^{+2} ions possess a primary hydration shell, which is the number of water molecules directly coordinated to both the metal ions. There is also overall solvation number, which is defined as the total number of water molecules associated when the solvent is water, on which both the ions exercise a substantial restraining influence. Then the successive layers of water molecules are termed as the secondary hydration layers. Hydration of an ion depends on the electrostatic attraction of water molecules to that ion. Attraction of water molecules around an ion depends on the density of charge of ion. The smaller ions having greater ionic potential attract more water molecules. The result is the inverse relationship between non-hydrated radius and hydrated radius. In this study, the non-hydrated radius of Pb^{+2} is 1.19 Å and second ionization potential is 15.028 eV while the same quantities for Fe^{+2} are 0.55 Å and 16.18 eV, respectively. Therefore, the reverse nature is observed for hydrated radii of Pb^{+2} and Fe^{+2} than that for the non-hydrated ones [17,18]. As the hydrated radii of Pb^{+2} being smaller than the hydrated radii of Fe^{+2}, the Pb^{+2} ions enter into the reaction in higher concentration than Fe^{+2} ions, which is resulting higher concentration of Pb in grown crystals than Fe.

Mechanism of dendrite crystal growth was studied by Fujiwara and Nakajima [19]. Dendrite type growth morphology has been observed by several authors in the gel grown crystals, such as lead tartrate [20], cadmium tartrate [21], ammonium tartrate [22] and lanthanum tartrate [23]. In the present study to grow lead and iron mixed levo tartrate crystals, the supernatant ions of Pb^{+2} and Fe^{+2} slowly diffused into the gel medium where they react with inner tartrate anions. The crystal growth was started about two days after pouring the supernatant solution at the gel liquid interface in the form of a thin layer of very small crystalline particles. As the content of lead was increased in the supernatant solution, this layer became dense and thick with white crystals in dendrite form, which is shown in figure 1. The dendritic nature is found may be due to instability occurring in the diffusion reaction process as the rapid growth of crystals takes place in one direction. The lead tartrate crystals are white and dendrite in shape while iron tartrate crystals are greenish brown and dark brown and spherulitic in nature [24]. But the dendrite form of the mixed lead and iron levo tartrate crystals is due to much higher wt % of lead in the grown crystals than iron.

A. FTIR Study

The FTIR spectra of the grown crystals for the samples I-III are shown the fig 2. The observed vibrational frequencies and their assignments are listed in the table 1. It can be observed from the spectra that the band nearly 3380 cm^{-1} is due to O-H stretching and water of crystallization. The bands observed at slightly less than 1600 cm^{-1} and near 1380 cm^{-1} are due to C=O stretching and C-H bending of alkane, respectively. The absorption

ISSN: 2277-3754
ISO 9001:2008 Certified
International Journal of Engineering and Innovative Technology (IJEIT)
Volume 4, Issue 1, July 2014

band nearly 1125 cm^{-1} and 835 cm^{-1} are due to C-O stretching and C-C banding, respectively. The absorption occurring nearly 2930 cm^{-1} is due to asymmetrical C-H stretching and the absorption taking place around 2632 cm^{-1} is due to bonded O-H stretching. The absorptions bands found between 500 and 700 cm^{-1} are due to the metal -oxygen bonding vibration. It can be seen from the table 1 that the composition of iron and lead in the mixed tartrate crystals does not have significant effect on various absorptions in FTIR spectra. In the pure lead tartrate crystal, the absorption corresponding to O–H stretching vibration occurs at 3384.9 cm^{-1} [12], while in the present mixed crystals containing different proportions of iron and lead this absorption occurs at 3380 cm^{-1}. It is found that the absorptions occur in lead and iron mixed levo tartrate crystals at nearly the same wave number that of the pure lead tartrate crystals. The O-H stretching vibration occurs in pure iron tartrate at 3540 cm^{-1} [24]. Further, this suggests that the O-H stretching vibration of iron tartrate has no influence in the O-H stretching vibration of lead and iron mixed levo tartrate due to very less concentration of iron present in the crystals. There is no significant effect on other absorptions in FTIR spectra.

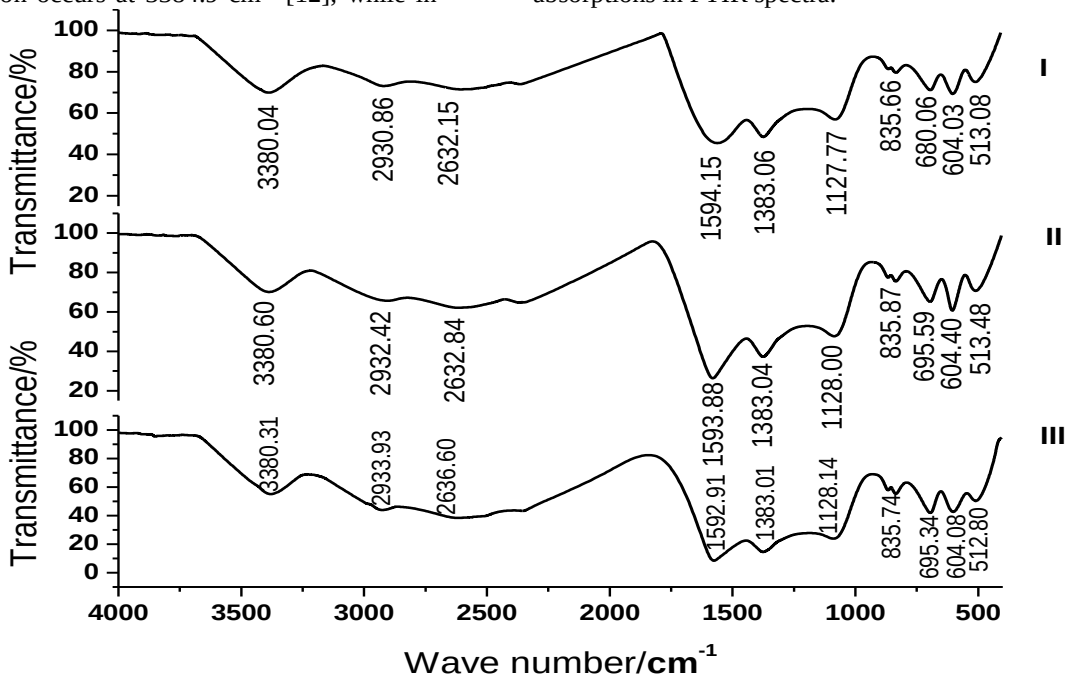

Fig 2. FTIR spectra of sample (I-III)

Table 1. Assignments for different absorptions in FTIR spectra for sample (I-III)

Assignments	Wave number (cm^{-1})		
	Sample (I)	Sample (II)	Sample (III)
Free O-H Stretching	3380.04	3380.60	3380.31
C-H Stretching (asymmetrical)	2930.86	2932.42	2933.93
Bonded O-H Stretching	2632.15	2632.84	2936.60
C=O Stretching	1594.15	1593.88	1592.91
C-H banding (Alkane)	1383.06	1383.04	1383.01
C-O Stretching	1127.77	1128.00	1128.14
C-C Bending	835.66	835.87	835.74
Pb-O and Fe-O Stretching	680.06, 604.03, 513.08	695.59, 604.40, 513.48	695.34, 604.08, 512.80

ISSN: 2277-3754
ISO 9001:2008 Certified
International Journal of Engineering and Innovative Technology (IJEIT)
Volume 4, Issue 1, July 2014

B. Powder XRD Study

The powder XRD patterns of the grown crystals for the samples I-III are shown the fig 3. The unit cell parameters were computed by using computer software Powder-X and are given in table 2. The orthorhombic unit cell parameters of lead tartrate crystals are: a = 7.99482 Å, b = 8.84525 Å, c = 8.35318 Å with space group $P2_12_12_1$ [25], while the orthorhombic unit cell parameters of iron tartrate crystals are a = 8.7588 Å, b = 10.9889 Å, c = 8.1900 Å [13]. Comparing with the pattern of pure lead tartrate, it is observed that the intensity of all the peaks of mixed crystals of Pb and Fe is reduced without significant change in the peak position of the pattern of pure lead levo tartrate. The scattering intensities for X-rays are directly related to the number of electrons in the atom. Hence, light atoms scatter X-rays weakly, while heavy atoms scatter X-rays more effectively. Therefore, doping of light element i.e. Fe, reduces the intensity of peaks. The percentage weight of iron in the structure of mixed crystals of lead and iron is very less and therefore, the unit cell parameters of mixed crystals are close to the unit cell parameters of pure lead. It is also observed that the most intense peaks of pure lead levo tartrate (020) at 21.12°, (022) at 29.44°, (031) at 32.25°, (131) at 34.17°, (311) at 36.25°, (040) at 40.88°, (033) at 44.71°, and (261) at 68.79° are shifted very little from their position. This indicates that there is no strain produced in the structure of pure lead tartrate due to doping of iron because of low ionic radius of iron (0.55 Å) compared to lead (1.19 Å) [26]. The peaks of Fe are not separately identified in the mixed crystals of Pb and Fe, which may be due to very less percentage of iron in the mixed crystals. From table 2, one can find that all the three samples I-III exhibit orthorhombic structure. The unit cell parameter values of lead and iron mixed tartrate crystals is closer to the unit cell parameters values of pure lead tartrate, which indicates that the less amount of iron in the mixed crystals has no significant influence on the unit cell dimensions.

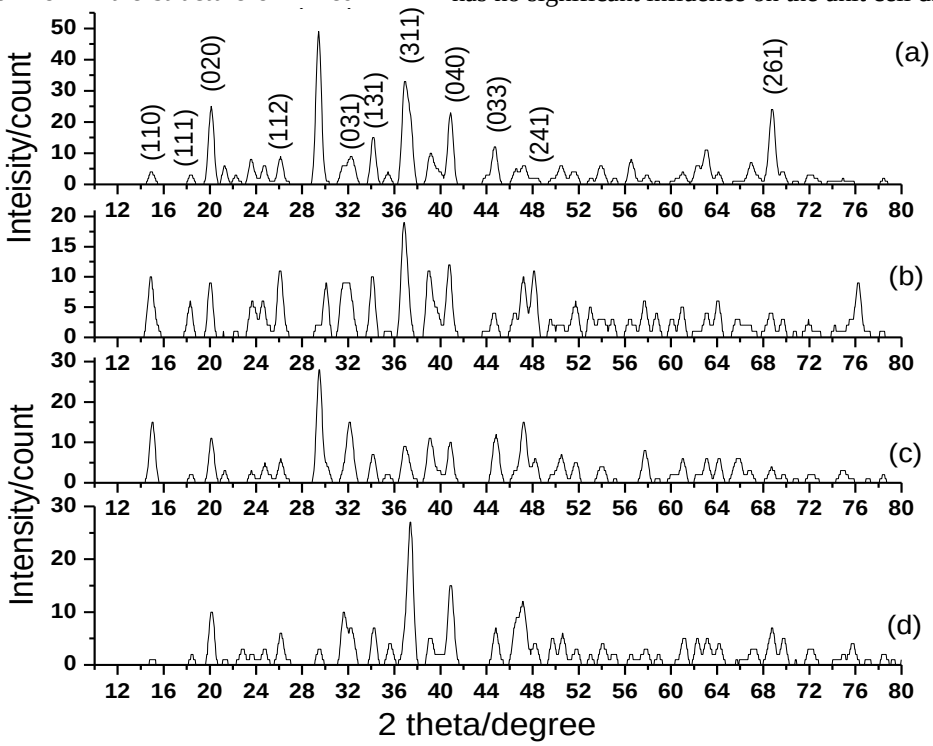

Fig 3. Powder XRD patterns (a) pure lead tartrate (b) sample I (c) sample II (d) sample III

Table 2. Unit cell parameters and crystal systems for sample (I-III)

Sample Name	Unit cell parameters	System
Sample (I)	a = 8.0048 Å , b = 8.8452 Å, c = 8.3532 Å	Orthorhombic $\alpha = \beta = \gamma = 90^o$
Sample (II)	a = 7.9820 Å , b = 8.8400 Å , c = 8.3550 Å	Orthorhombic $\alpha = \beta = \gamma = 90^o$
Sample (III)	a = 7.9920 Å , b = 8.8500 Å , c = 8.3540 Å	Orthorhombic $\alpha = \beta = \gamma = 90^o$

ISSN: 2277-3754
ISO 9001:2008 Certified
International Journal of Engineering and Innovative Technology (IJEIT)
Volume 4, Issue 1, July 2014

C. Thermal behavior

There are reports available in literature on thermal studies on metal tartrate systems, for example, iron-manganese levo tartrate [13], ternary iron-manganese-cobalt tartrate compound [15] as well as ternary iron-manganese-nickel tartrate compound [16]. Fig 4 shows the thermo-gram for the samples I-III.

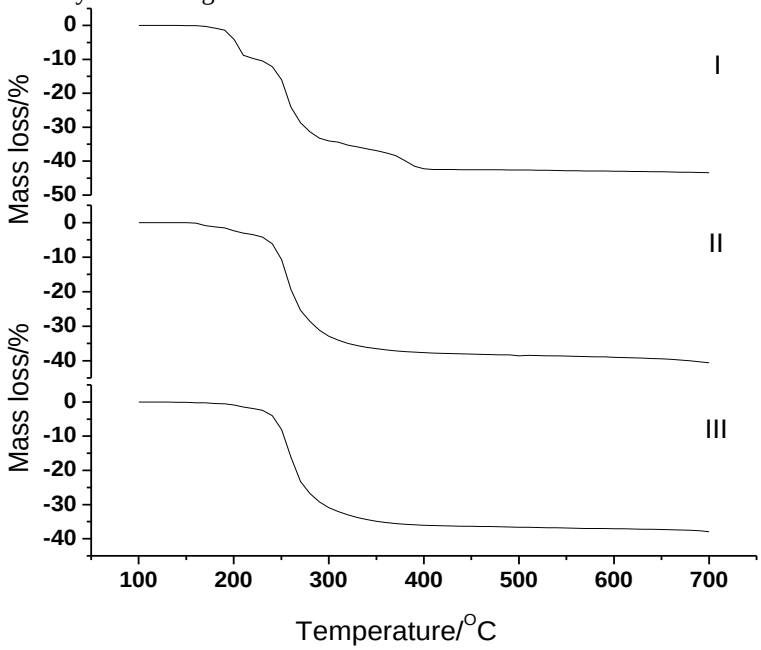

Fig 4. TG curves of sample (I-III)

For the sample (I), the first stage of dehydration occurs between 170 and 210°C, which results into formation of anhydrous lead-iron mixed tartrate. During the second stage between 210 and 280°C, the anhydrous sample is converted into carbonate form. During the third and final stage of decomposition between 280 and 400°C, the sample is converted into oxide form. The similar behavior is found for sample II and sample III.

Table (3) gives details of the thermal decomposition of the samples (I-III) with theoretically calculated and experimentally obtained mass loss values. The amount of water molecules attached with samples (I, II and III) have been calculated and found to be 1.9, 0.5 and 0.17, respectively. The correct stoichiometric formula for the crystals of all the samples I-III is $Pb_{98.93}Fe_{1.07}C_4H_4O_6$ $1.9H_2O$, $Pb_{99.36}Fe_{0.64}C_4H_4O_6$ $0.5H_2O$ and $Pb_{99.38}Fe_{0.62}C_4H_4O_6$ $0.17H_2O$, respectively.

Table 3. Theoretical and experimental mass loss values for sample (I-III)

Sample name	T (°C)	Reactions involved	Theoretical mass (%) calculated	Experimental mass (%/) from graph
Sample (I)	50-170	No decomposition	100	100
	170-210	$Pb_{98.93}Fe_{1.07}C_4H_4O_6$ $1.9H_2O \rightarrow Pb_{98.93}Fe_{1.07}C_4H_4O_6 + 1.9H_2O$	8.83	8.77
	210-280	$Pb_{98.93}Fe_{1.07}C_4H_4O_6 \rightarrow Pb_{98.93}Fe_{1.07}\ CO_3 + CH_4 + 2CO + 1/2O_2$	31.53	31.32
	280-400	$Pb_{98.93}Fe_{1.07}\ CO_3 \rightarrow Pb_{98.93}Fe_{1.07}O + CO_2$	42.89	42.27
Sample (II)	50-160	No decomposition	100	100
	160-200	$Pb_{99.36}Fe_{0.64}C_4H_4O_6$ $0.5H_2O \rightarrow Pb_{99.36}Fe_{0.64}C_4H_4O_6 + 0.5H_2O$	2.48	2.40
	200-270	$Pb_{99.36}Fe_{0.64}C_4H_4O_6 \rightarrow Pb_{99.36}Fe_{0.64}\ CO_3 + CH_4 + 2CO + 1/2O_2$	26.72	25.40
	270-400	$Pb_{99.36}Fe_{0.64}\ CO_3 \rightarrow Pb_{99.36}Fe_{0.64}O + CO_2$	38.84	37.66

ISSN: 2277-3754
ISO 9001:2008 Certified
International Journal of Engineering and Innovative Technology (IJEIT)
Volume 4, Issue 1, July 2014

Sample (III)	50-160	No decomposition	100	100
	160-200	$Pb_{99.38}Fe_{0.62}C_4H_4O_6\ 0.17H_2O \rightarrow Pb_{99.38}Fe_{0.62}C_4H_4O_6 + 0.17H_2O$	0.86	0.89
	200-280	$Pb_{99.38}Fe_{0.62}C_4H_4O_6 \rightarrow Pb_{99.38}Fe_{0.62}\ CO_3 + CH_4 + 2CO + 1/2O_2$	25.50	26.77
	280-400	$Pb_{99.38}Fe_{0.62}\ CO_3 \rightarrow Pb_{99.36}Fe_{0.64}O + CO_2$	37.83	36.07

Fig 5 shows the DTA plot of samples I-III. For the sample I the decomposition process occurs through two exothermic reactions at 304.9°C and 414.0°C, respectively. For the first exothermic reaction at 304.9°C the enthalpy and the change in heat capacity are calculated and found to be 777.92 J g^{-1} and 3.754 J g^{-1} K^{-1}, respectively. This strong exothermic reaction at 304.9°C may be due to decomposition of sample into carbonate form. For the second exothermic reaction at 414.0°C the enthalpy and the change in heat capacity are calculated and found to be 93.84 J g^{-1} and 4.260 J g^{-1} K^{-1}, respectively. This exothermic reaction at 414.0°C may be due to occurrence of oxidative process accompanying decomposition.

For the sample (II) also, the decomposition process occurs through two exothermic reactions at 301.4°C and 429.6°C, respectively. The enthalpy and the change in heat capacity are evaluated for the first exothermic reaction at 301.4°C and found to be 726.05 J g^{-1} and 1.760 J g^{-1} K^{-1}, respectively. The exothermic reaction at 301.4°C may be due to decomposition of sample into carbonate form. With comparison to sample (I) the thermodynamic parameter values are less for this carbonate stage reaction, which also indicates meta-stable or briefly stable carbonate stage in the sample (II). The enthalpy and the change in heat capacity are calculated for the second exothermic reaction at 429.6°C and found to be 86.75 J g^{-1} and 3.389 J g^{-1} K^{-1}, respectively. This strong exothermic reaction at 429.6°C may be due to occurrence of oxidative process accompanying decomposition.

The decomposition process for the sample (III) occurs through two exothermic reactions at 315.9°C and 421.5°C, respectively. For the first exothermic reaction at 315.9°C the enthalpy and the change in heat capacity are found to be 1361.33 J g^{-1} and 10.316 J g^{-1} K^{-1}, respectively. This exothermic reaction may be due to decomposition of sample into carbonate form. With comparison to sample I and II, the thermodynamic parameter values are high for this carbonate stage reaction, which indicates unstable carbonate stage in the sample (III). For the second exothermic reaction at 421.5°C the enthalpy and the change in heat capacity are found to be 101.08 J g^{-1} and 2.392 J g^{-1} K^{-1}, respectively. This exothermic reaction may be due to occurrence of oxidative process accompanying decomposition. Comparing different parameters of all the three samples, it can be concluded that as the % weight of iron is increased in the sample, the stable carbonate stage is obtained.

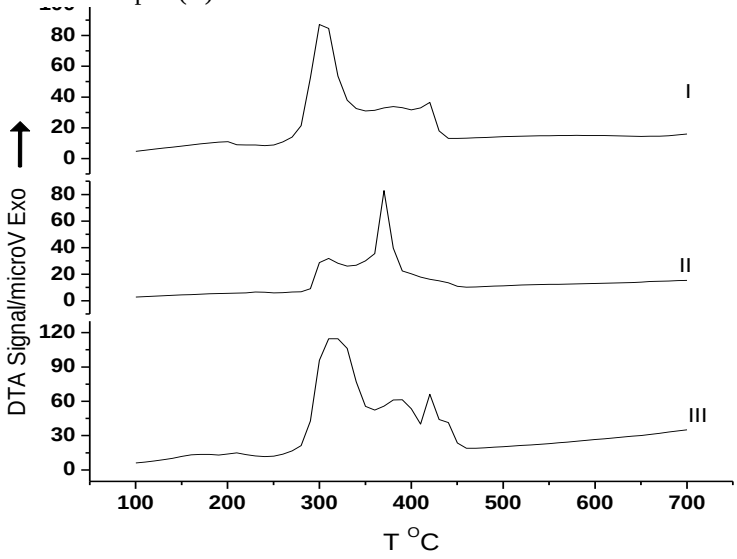

Fig 5. DTA curves of sample (I-III)

ISSN: 2277-3754
ISO 9001:2008 Certified
International Journal of Engineering and Innovative Technology (IJEIT)
Volume 4, Issue 1, July 2014

IV. CONCLUSIONS

The lead-iron mixed levo tartrate crystals with different compositions were grown in silica gel by using the mixture of lead nitrate and iron nitrate nonahydrate as supernatant solutions in different amounts. The EDAX analysis suggested that iron enters into lattice in less amount with comparison to lead, which is due to the higher hydrated radius of Fe^{+2} ions compared to Pb^{+2} ions. The FTIR spectra of the grown crystals indicated the presence of O-H, C-H, C-O, C=O and C-C functional groups with metal-oxygen vibrations. The powder XRD suggested the orthorhombic crystal structure of all the three samples, indicating the nature of parent compound lead levo tartrate persists in the mixed lead iron levo tartrate crystals. From the thermo-grams it was found that the crystals were thermally unstable. On heating they became anhydrous and decomposed into metal oxides through a single stage of carbonate. From DTA two exothermic reaction stages were identified corresponding to carbonate and oxidative stages. Various thermodynamic parameters were evaluated from DSC. The presence of water molecules was detected and calculated. The exact chemical formulations for mixed crystals were suggested.

ACKNOWLEDGMENT

The authors are thankful to Prof. H.H. Joshi (HOD, Physics) for his keen interest and the author (HOJ) is thankful to the Principal and the Management of Maharaja Shree Mahendrasinhji Science College, Morbi for encouragements.

REFERENCES

[1] Lebioda, Lukasz, Jakob and Clarissa G (1998) Treating prostate cancer with tartrate ions, United States Patent 5763490.

[2] Sprument P and Musy J (1971) pH effect on electron microscopical contrast solutions. Histochemie 26(3):228-37.

[3] Weber G (1991) Speciation of iron using HPLC with electrochemical and flame-AAS detection Fresenius, J Anal Chem 340:161-65.

[4] Strebel R, Vasku J and Selye H (1962) Comparative study of the calciphylactic challenging potency of various iron compounds, J Pharm Pharmocol 14:658-63.

[5] Clark AC, Dias DA, Smith TA, Ghiggino KP and Scollary GR (2011) Iron (III) tartrate as a potential precursor of light-induced oxidative degradation of white wine: Studies in a model wine system, J Agric Food Chem 59(8):3575-81.

[6] Sahaya Shajan X and Mahadevan C (2005) FTIR spectroscopic and thermal studies on pure and impurity added calcium tartrate tetra hydrate crystals, Cryst Res Technol 40(6):598.

[7] Hopwood JS and Nicol AW (1972) Crystal data of cadmium tartrate pentahydrate, Crystallogr J Online 5:1600-5767.

[8] Rahway NJ (1952) The Merck index of chemicals and drugs. 6th ed. Merck and Co.

[9] Henish HK (1993) Crystal growth in gels Dover New York

[10] Dabhi RM and Joshi MJ (2003) Thermal studies of gel grown cadmium tartrate crystals, Indian J Phys 77:481-5.

[11] Joseph S, Joshi HS and Joshi MJ (1997) Infrared spectroscopic and thermal studies of gel grown spherulitic crystals of iron tartrate, Cryst Res Technol 32(2):339-46.

[12] Jethva HO and Parsania MV (2010) Growth and characterization of lead tartrate crystals, Asian J Chem 22(8):6317-20.

[13] Joshi SJ, Parekh BB, Parikh KD, Vora KD and Joshi MJ (2006) Growth and characterization of gel grown pure and mixed iron-manganese levo-tartrate crystals, Bull Mater Sci 29(3):307-12.

[14] Parikh KD, Parekh BB, Dave DJ and Joshi MJ (2006) Investigation of various growth parameters, FTIR and thermal studies of gel grown pure and mixed levo-tartrates of calcium and strontium, Indian J Phys 80(7):719-26.

[15] Joshi SJ, Tank KP, Parekh BB and Joshi MJ (2010) Characterization of gel grown iron-manganese-cobalt ternary levo-tartrate crystals, Cryst Res Technol 45:303-10.

[16] Joshi SJ, Tank KP, Parekh BB and Joshi MJ (2012) FTIR and thermal studies of iron-nickel-manganese ternary levo-tartrate crystals, J Therm Anal Calorim 10.1007/s10973-012-2624-8.

[17] Dove and Nix (1997) Ionic hydration in chemistry and biophysics, Geochim Cosmochim Acta 61:3331.

[18] Albert CF, Wilkinson G, Gaus PL (1995) Basic Inorganic Chemistry 3rd ed. Wiley, Singapore.

[19] Fujiwara K and Nakajima K (2009) Mechanism of dendritic crystal growth, Springer.

[20] Abdulkadhar M and Ittyachen MA (1977) Development of lead tartrate crystals from its dendritic form, J Cryst Growth 39:365.

[21] Dabhi RM, Parekh BB and Joshi MJ (2005) Dielectric studies of gel grown zinc tartrate crystals, Indian J Phys 79(5):503.

[22] Saraf AD, Saraf KB, Wani PA and Bhoraskar SV (1986) Dendrititc growth of ammonium tartrate single crystals in silica gel, Cryst Res Technol 21(4):449.

[23] Kotru PN, Gupta NK and Raina KK (1986) Growth of lanthanum tartrate crystals in silica gel, J Mater Sci 21:90.

[24] Joseph S (1997) Growth and characterization of some ionic crystals. Ph D Dissertation, Saurashtra University, Rajkot, India.

[25] De Ridder DJA, Goubitz K, Sonneveld EJ, Molleman W and Schenk H (2002) Lead tartrate from x-ray powder diffraction data, Cryst Struct Commun C58:m596-8.

[26] Cullity BD (1978) Elements of x-ray diffraction. Addison-Wesley.